Composition and size tailored synthesis of iron selenide nanoflakes†

Liqiao Chen,[ab] Hongquan Zhan,[a] Xianfeng Yang,[a] Zhaoyong Sun,[b] Jun Zhang,[b] Dan Xu,[b] Chaolun Liang,[a] Mingmei Wu*[a] and Jiye Fang*[b]

Received 13th April 2010, Accepted 16th June 2010
DOI: 10.1039/c005097k

Regular square $FeSe_x$ nanoflakes with tetragonal PbO-type phase and selenium deficiency have been grown from an inorganic iron source, *i.e.* ferrous chloride and selenium trioctylphosphine through a simple solution-based route in the co-solvent of oleylamine and oleic acid. The phase and structure are identified by powder X-ray diffraction and electron microscopy. The square nanoflakes are revealed to be bound by two larger {001} planes and four equivalent smaller {100} side surfaces. The appearance of the larger {001} planes and flaky morphology inherently results from the greatest atom density on {001} lattice planes and the largest d_{001} spacing. The addition of the organic acid, *i.e.* oleic acid, at a proper stage during heating of the starting materials, is of great importance to the yield of the tetragonal PbO-type phase. Interestingly, the chemical composition and the edge length of the single crystalline $FeSe_x$ nanoflakes can be tailored readily by using an organic diol which is suggested to serve as a reducing agent and chemical ligand. Thus, the deficiency of selenium can be highly reduced and the top-bottom surface area be enlarged.

1. Introduction

The preparation of a solid state material with a desired crystal phase and chemical component is of crucial importance in traditional solid chemistry.[1] Solution chemistry as a simple route can yield a range of nanocrystals with tunable sizes and variable shapes. Because many unique physical and chemical properties are highly size and/or shape dependent, the controlled growth of nanocrystals *via* solution chemistry has received intensive research interest in nanochemistry.[2] In addition, a specific phase can be readily achieved by modifying growth conditions through solution chemistry.[3] Tetragonal PbO-type β-$FeSe_x$ represents a kind of interesting material that has been proven to have potential in many fields due to its magnetic,[4–6] electrochemical,[7] optical and electrical properties.[8,9] Significantly, the discovery of its superconductivity[10] has generated more and more attention towards the preparations, structures, and properties of the family with composition modification in $FeSe_{1-y}$.[11–19] Both experimental and theoretical studies show that the superconductivity and other physical properties are highly dependent on selenium deficiency deviated from the ideal stoichiometry of FeSe.[10–12] In addition, strong orientation and thickness-dependent superconductivity have been investigated for $FeSe_x$ thin films with preferred orientation growth,[14] further indicating crystal-size and growth-orientation effects.[15] Therefore, it is of great importance to synthesize phase-pure tetragonal $FeSe_x$ samples with tunable compositions, sizes and even shapes.

Many groups have been challenging the controlled growth of β-$FeSe_x$ with tetragonal phase, designed deficiencies, and specified sizes. Firstly, besides the tetragonal phase with PbO structure, $FeSe_x$ appears in several other phases, such as a hexagonal NiAs-type phase with a wide range of compositions showing a transformation from hexagonal (*e.g.* FeSe and Fe_7Se_8) to monoclinic (*e.g.* as Fe_3Se_4) symmetry, and orthorhombic marcasite structured $FeSe_2$.[15,20] Secondly, although the synthesis of $FeSe_x$ bulk materials with tunable x values has been well and extensively documented, the preparations are generally carried out at high temperature *via* solid-state reaction,[12,17] a flux growth method,[18] and vapor self-transport.[19] Thirdly, besides economically prohibitive high temperatures, meticulous conditions, sophisticated facilities, inert and refractory substrates are required during the growth of β-$FeSe_x$ thin films by using chemical vapor deposition (CVD),[5] pulsed laser deposition[6] and molecular beam epitaxy (MBE).[7] Actually, these routes can not be developed as a feasible way to yield size and shape tunable single crystals.

Solution-based chemical routes can allow for monodisperse and shape-controllable crystal growth under facile conditions.[2] Previously, orthorhombic $FeSe_2$ nano- and micro-crystals, *i.e.* a non-tetragonal phase, had been grown *via* solvothermal routes.[16] Recently, predominantly two-dimensional $Fe_{0.994}Se_{1.014}$ nanosheets have been reported by Raymond E. Schaak and his colleagues, who adopted $Fe(CO)_5$ as an iron source and trioctylphosphine oxide (TOPO) as solvent.[15] This is an important progression in the successful growth of $FeSe_x$ *via* solution chemistry. However, the $FeSe_x$ sample was not Se-deficient and the tailoring of chemical composition and size have not been realized so far. Herein, we present a new wet-chemical strategy in the growth of much more uniform tetragonal β-$FeSe_x$ square nanoflakes with tunable composition and size, in which iron

[a]*MOE Key Laboratory of Bioinorganic and Synthetic Chemistry/State Key Laboratory of Optoelectronic Materials and Technology, School of Chemistry and Chemical Engineering, Instrumental Analysis and Research Centre, Sun Yat-Sen (Zhongshan) University, Guangzhou, 510275, P. R. China. E-mail: ceswmm@mail.sysu.edu.cn; Fax: +86-20-84111038; Tel: +86-20-84111823*
[b]*Department of Chemistry, State University of New York at Binghamton, Binghamton, New York, 13902, USA. E-mail: jfang@binghamton.edu; Fax: +1-607-7774478; Tel: +1-607-7773752*

† Electronic supplementary information (ESI) available: Additional XREDS spectra and a TEM image. See DOI: 10.1039/c005097k

chloride ($FeCl_2$) was used as an iron source, oleylamine as solvent, and a small amount of oleic acid as co-solvent.

2. Experimental

Chemical Synthesis

All chemicals were received from Sigma-Aldrich without further purification. In a typical synthesis of tetragonal β-$FeSe_x$ nanoflakes, 38 mg (0.3 mmol) of $FeCl_2$, 7.5 mL of oleylamine (70%) were loaded into a three-neck round-bottom flask equipped with a condenser. The mixture was heated up to 110 °C with mild stirring and was gradually vacuumed. Standard air-free techniques was used. After the temperature reached 110 °C, 0.5 mL of oleic acid (90%) was then added into the mixture under vigorous agitation. After the system was further vacuumed for 15 min at 110 °C, the temperature was increased to 130 °C and 0.3 mL of pre-prepared selenium trioctylphosphine (Se-TOP) solution (90% for TOP, 1.0 mol L^{-1} for Se) was rapidly injected under an argon stream. The mixture was subsequently heated to 320 °C and refluxed for 20 min. During this heating stage, the color of the mixture turned black at about 305 °C. For the case with the presence of 1,2-tetradecanediol (TDD), TDD was added together with $FeCl_2$ into a three-neck round-bottom flask and the reaction could be conducted at 300 °C, which also reduces the probable evaporation of TDD. The system was cooled down to room temperature, and the resultant black precipitates were isolated by adding sufficient amounts of a mixture of anhydrous ethanol and hexane and collected by subsequent centrifugation. The as-obtained black samples were dried in a vacuum oven at room temperature.

Characterization

Samples were characterized using a PAN analytical X-ray diffractometer (X'Pert system) equipped with a Cu $K\alpha 1$ radiation source ($\lambda = 0.15406$ nm), a scanning electron microscope (SEM), transmission electron microscope (TEM), and high-resolution TEM (HRTEM). SEM images were taken with a FEI Quanta 400 Thermal FE Environment Scanning Electron Microscope. Samples were gold-coated prior to the SEM analysis. TEM images were prepared on a JEM-2010HR transmission electron microscope operated at an accelerating voltage of 200 kV. The microscope was equipped with an Oxford EDS spectrometer and Gatan GIF Tridiem systems for both structural and chemical analysis. TEM samples were prepared by dispersing the powders on holey carbon film supported on copper grids.

3. Results and discussion

Structural characterization

The typical product generated from the reaction of anhydrous $FeCl_2$ and selenium in the organic solvent with absence of TDD was checked by powder X-ray diffraction (pXRD) (Fig. 1), electron micrography and electron diffraction (Fig. 2a–c). The pXRD pattern in Fig. 1 matches well with the JCPDS card No. 85-0735 for tetragonal $FeSe_x$ with $a = b = 0.3765$ and $c = 0.5518$ nm, confirming that the product was PbO-type $FeSe_x$ ($P4/nmm$).[10] This indicates that phase-pure tetragonal β-$FeSe_x$ could be grown by using such a simple inorganic iron source.

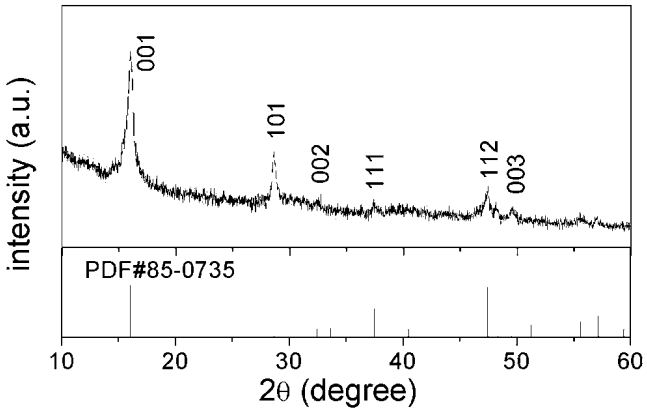

Fig. 1 Powder X-ray diffraction pattern of the product obtained through the typical growth procedure. The bars are from JCPDS card No. 85-0735 for tetragonal β-FeSe.

According to the theory of Curie and Wulff ,[21] a free crystal of tetragonal $FeSe_x$ should have a plate morphology due to the large d-spacing of 001. The TEM images of the dispersed β-$FeSe_x$ particles show that they are all crystallized in square flakes with edge length around 110 nm and thickness around 8 nm (Fig. 2a,c). The fast Fourier transformation (FFT) pattern (Fig. 2b, insert) and its corresponding HRTEM image with defined lattice fringes taken from one part of a nanoflake as denoted inside the white square (Fig. 2c) indicate its zone axis is along the [001] direction when it is lying horizontally. The selected area electron diffraction (SAED) pattern (Fig. 2c, insert) from the entire nanoflake suggests its single crystalline nature and further manifests that it is enclosed by two ±(001) and four equivalent {100} lattice planes as larger top-bottom and thinner side surfaces, respectively (Fig. 2c). The highly retarded growth along the c-direction and the enhanced one along (001) planes are rationalized by the inherent layer crystal structure of FeSe as described previously (Fig. 2d).[15] As presented in Fig. 2d, the covalently bonded Fe and Se slabs vertically stack together along the c-axis *via* van der Waals forces in (001) planes. The significantly improved intensity of the 001 diffraction peak in pXRD (Fig. 1) reveals a preferred orientation of the as-synthesized crystals, which is consistent with the results from TEM images and the related FFT pattern (Fig. 2a–c).

Influence of the addition procedure of oleic acid on the growth

The mixture of oleylamine and oleic acid has been extensively used as a co-solvent, reducing agent and/or surfactant in the controlled growth of monodispersed nanocrystals.[2,22] An optimized use of each of them is quite essential in a successful growth of target nanocrystals. The sequence of the addition of the solvent pair has an important influence on the nucleation and growth of nanocrystals.[22] As described in the experimental section, oleic acid was added after the temperature reached 105 °C and the mixing of $FeCl_2$ into oleylamine (70%). If 0.5 mL of oleic acid was mixed with oleylamine at ambient temperature before heating, the target tetragonal phase was hardly yielded (Fig. 3a). After the temperature of the mixture of $FeCl_2$ and

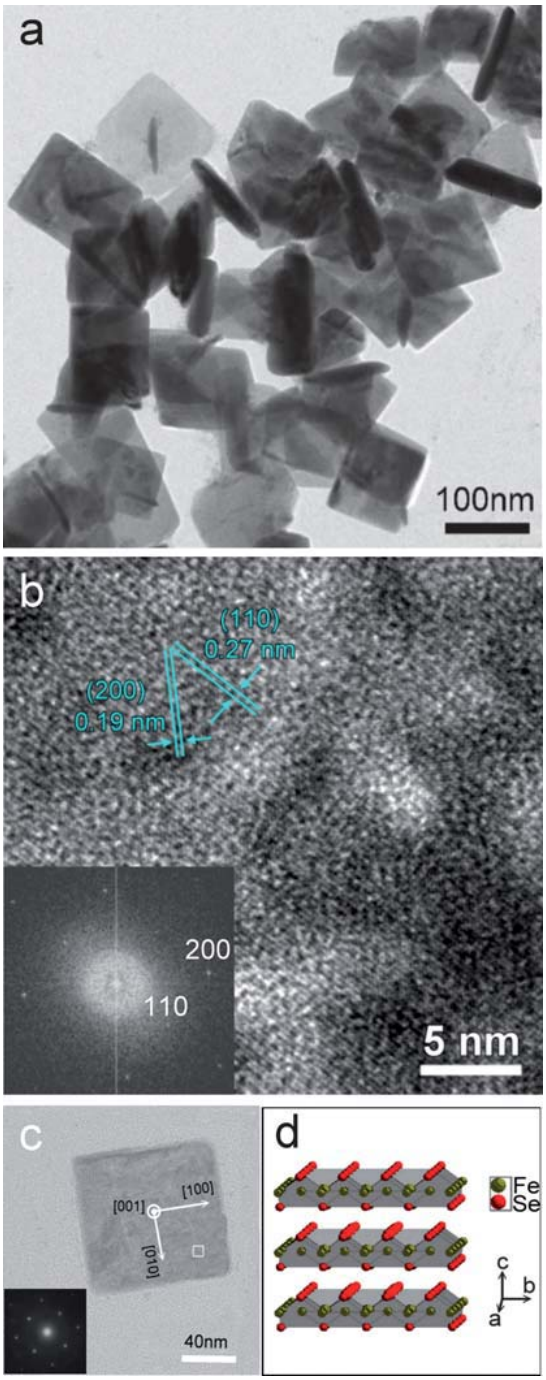

Fig. 2 (a) Low magnification, (b) high resolution TEM images with inserted FFT pattern. (c) A single nanoflake and its SAED pattern with [001] zone axis and (d) a schematic layer structure model.

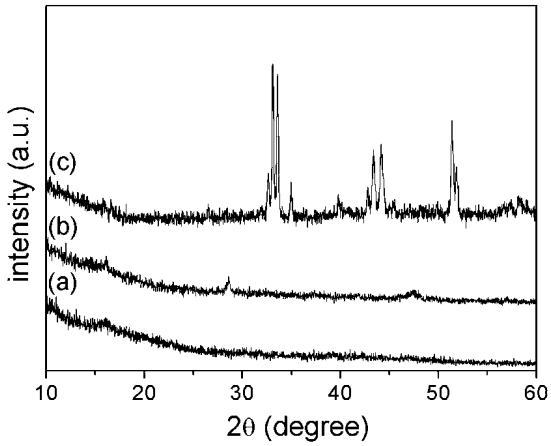

Fig. 3 Powder X-ray diffraction patterns of the products obtained with slightly modified conditions compared to the typical procedure as shown in Fig. 1. (a) Adding oleic acid (0.5 mL) into the mixture of $FeCl_2$ and oleylamine (7.5 mL) at ambient temperature, and (b) at 60 °C, respectively. (c) Mixing oleic acid (7.5 mL) with $FeCl_2$ first at ambient temperature and then adding oleylamine (0.5 mL) at 110 °C.

oleylamine reached 60 °C at the first stage, 0.5 mL of oleic acid was then added under vigorous agitation, the as-obtained product can be identified as a pure tetragonal phase but poorly crystallized as suggested by its powder XRD pattern (Fig. 3b). Interestingly, instead of oleylamine, 7.5 mL of oleic acid was used as solvent for $FeCl_2$ and then instead of oleic acid, 0.5 mL of oleylamine was added after heating to 110 °C in the typical growth procedure, monoclinic Fe_3Se_4 (JCPDS card No.71-2251) but not tetragonal $FeSe_x$ phase was generated (Fig. 3c). Thus, the addition of oleic acid should be carried out at a proper stage and a suitable temperature. It has been broadly accepted that the evolution of nanocrystals in a solution system consists of a nucleation stage and a subsequent Ostwald ripening growth on the existing seeds (or nuclei).[22a] The rates of nucleation and subsequent growth are the keys to well crystalline products and size/shape control. Oleic acid can serves as a ligand to form a complex with iron and thus its presence can control the state of iron in the starting mixture. In the absence of oleic acid, the resultant nanoflakes are not so uniform (see ESI†) as those in Fig. 2. However, the much earlier presence of oleic acid might reduce the nucleation and consequently retard the growth of $FeSe_x$. Thus, a poorly crystalline product is yielded if the oleic acid is added at a much earlier stage. However, the complexing ability between nitrogen atom in oleylamine to iron atom and oxygen atom in oleic acid to iron atom is different. Iron(II) can exist much more stably in amines than in organic acids. The earlier presence of oleic acid and absence of oleylamine can not preserve the state of the iron properly and thus other products are yielded (Fig. 3c).

Composition and size tailoring: the use of TDD

The relative molar ratio of Fe to Se in the typical product was checked briefly *via* SEM energy-dispersive X-ray spectroscopic (EDS) analysis from the whole stack of sample (Fig. 4), in which the nanoflakes are nearly uniformly dispersed. The percentages of Fe and Se are 65 at% and 35 at%, respectively, corresponding to a chemical formula of $FeSe_{0.54}$, indicating a considerable deficiency of selenium in the stoichiometry. The excess Fe is quite evident. An effort to increase the content of Se is necessary and practical. Previously, the product of $Fe_{0.994}Se_{1.014}$ with a slight excess of selenium was obtained by using $Fe(CO)_5$ as the iron source.[15] Herein, the relatively economic and safe $FeCl_2$ was adopted as the iron source and the growth approach was facile. In addition, nearly uniform particles have been generated by the present route. Significantly, the chemical composition and size

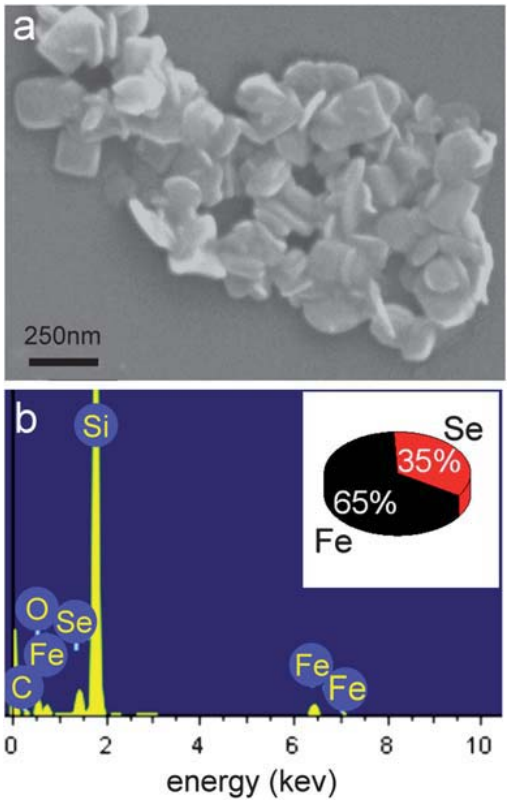

Fig. 4 (a) SEM image and (b) related EDS profile with resultant atom ratio as percentage in $FeSe_x$.

tailoring can be achieved *via* a general but unique route as will be described in this paper.

As reported in the literature, the superconducting property of tetragonal $FeSe_x$ bulk materials is dependent on the x value.[10–12] Therefore, the control and tuning of the chemical composition of $FeSe_x$ is of considerable importance to optimize physical performance. The tuning and modification of atom ratio in a product from solution chemistry is commonly realized by a ratio change of respective component in the starting feedstocks. In this work, however, we demonstrate a unique method to finely tune the chemical composition of $FeSe_x$ products without varying the amounts of source materials, *i.e.* iron and selenium sources. Instead, with an employment of an organic

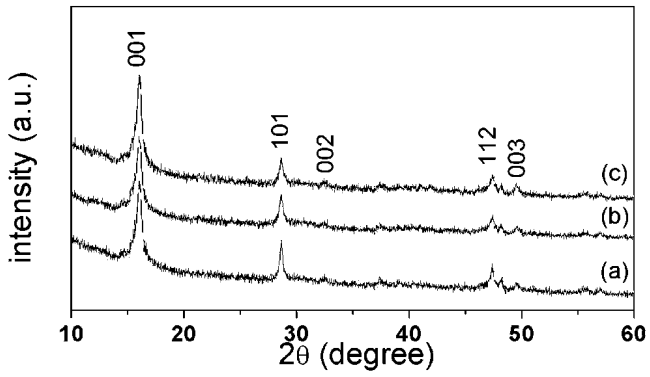

Fig. 5 Powder X-ray diffraction patterns of the products obtained after the addition of 0.07, 0.10 and 0.14 g of TDD.

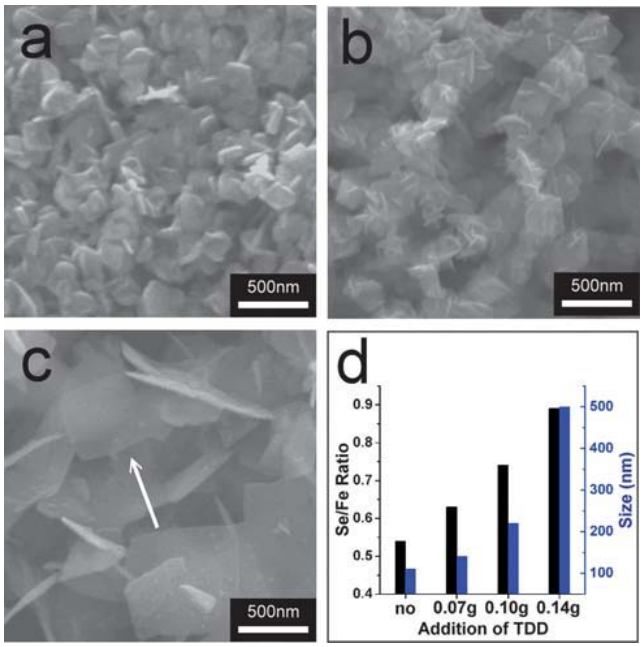

Fig. 6 SEM images of the products obtained with an addition of (a) 0.07, (b) 0.10 and (c) 0.14 g of TDD. (d) The Se/Fe ratio and larger crystal surface size in each product with a change in the addition of TDD (Fig. S2†).

diol, *i.e.* 1,2-tetradecanediol (TDD), compounds with higher Se components can be synthesized. TDD (1,2-tetradecanediol) has been widely used as a mild organic reducing agent to facilitate the nucleation process.[23] We accordingly shared this insight and employed TDD as a reducing agent. By addition of 0.07, 0.10 and 0.14 g of TDD into three reaction systems, three tetragonal $FeSe_x$ products could be obtained, respectively (Fig. 5 and 6). Interestingly, the chemical components of $FeSe_x$ can be tailored to be $FeSe_{0.63}$, $FeSe_{0.74}$ and $FeSe_{0.89}$, respectively, based on the EDS results (Fig. 6d and ESI†). The controlled growth of $FeSe_x$ with tunable composition is of great importance in the study of superconductivity. Unfortunately, the measurement of superconductivity has not been successful so far probably due to a limited size (thickness).[14,15]

In addition, the shape and size can be modified with the addition of TDD but the flaky shape is preserved. The larger surface area extends with a further addition of TDD. That is the top-bottom surfaces area of the nanoflakes increases in the presence of more TDD (Fig. 6). The ratios of larger ±(001) surface area to thickness tend to be remarkably increased but the square outline of the top-bottom surface remains (Fig. 6c, white arrows).

TDD plays an important role in controlling the growth, the size/shape and the composition. To understand this, we carefully looked into the experimental phenomenon during heating. There is a sudden change in the solution color from yellow to black observed in the heating process, which can be taken as a sign of the generation of $FeSe_x$ (Scheme 1). Without addition of TDD, a heating temperature up to 305 °C for a quick color change to black in the hot reaction solution was required. That is, tetragonal $FeSe_x$ nanoflakes that are black in color could be only formed at *ca.* 305 °C in the absence of TDD. This is further

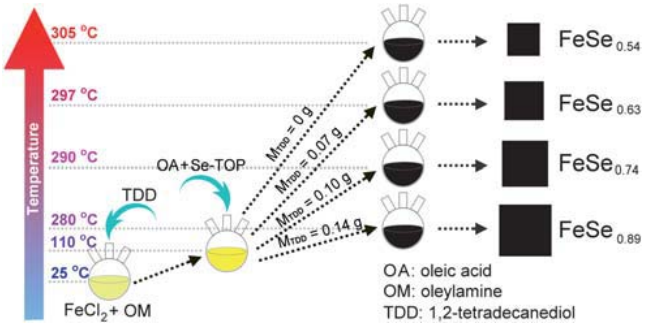

Scheme 1 A schematic illustration of the experimental procedures and results.

suggested by another experimental observation without the formation of black solid precipitates, in which the same reaction was conducted at 280 °C and even for 30 min. In the presence of 0.07, 0.10 or 0.14 g of TDD in a typical reaction system, however, a color change was obvious at 297, 290 or 280 °C, implying that TDD accelerates the initiation of $FeSe_x$.

Derived from our previous results for the synthesis of PtCu nanocrystals, in which TDD was an efficient reducing agent for promoting their growth,[23] a possible growth mechanism of $FeSe_x$ can be addressed in a similar way. Firstly, Se is from the decomposition of Se-TOP, which can be promoted at higher temperature. Secondly, TDD serves as a reducing agent which facilitates the reduction of Se to Se^{2-} ions as an "intermediate" for a subsequent formation of $FeSe_x$ between Se^{2-} and Fe^{2+}. In the absence of TDD, it would be more difficult to produce Se^{2-}, resulting in a higher Se deficiency due to the high stability of Se-TOP. As a consequence, with increasing amounts of TDD, the Se^{2-} content increases and the production is enhanced.

The evidence in Fig. 2b and c indicates that the larger up-bottom surfaces are bound by terminal {001} planes. The square flakes with two larger {001} surfaces becomes more apparent with increasing the addition of TDD (Fig. 6). It has been well accepted that the crystal growth rate along a crystallographic orientation is proportional to the surface attachment energy. Generally spoken, a small surface attachment is associated with a large *d*-spacing, herein the largest one is attributed to 001. Since the crystal growth along the <001> direction is the slowest, a free crystal of tetragonal $FeSe_x$ should have square flake morphology as described above (Fig. 2c). As the atom density on (001) lattice plane is greater than others on (100), (101) and (111) ones, the enhanced growth along the (001) planes can certainly enlarge the top-bottom surface on each nanoflake. Due to the deficiency at Se sites and the presence of extra positively-charged Fe^{2+} atoms on the (001) plane, TDD molecules can coordinate Fe^{2+} and be adsorbed on (001) planes. With the increase of TDD, the growth along the <001> direction is significantly retarded and flaky nanostructures with larger (001) surfaces are achieved (Fig. 6 and Scheme 1).

4. Conclusions

In summary, PbO-type tetragonal $FeSe_x$ nanoflakes enclosed by two ±(001) lattice planes as top-bottom surfaces and four {100} as side planes have been grown through a solution route by using a simple and safe inorganic iron precursor. The successful growth of the target product is not only dependent on the component of the starting materials[22,23] but the addition procedure of some feedstocks such as the addition of oleic acid herein. The presence of TDD in the reaction system can favor the growth of β-$FeSe_x$ and result in the production of β-$FeSe_x$ nanoflakes with larger top-bottom {100} surfaces and with higher Se component. This will provide a general growth route to tailor chemical composition, size and shape, and even to optimize the physical performance of nanocrystals.

Acknowledgements

This work is supported financially by the National Natural Science Foundation (NSF) of China and the Government of Guangdong Province for NSF (Grants U0734002, 50872158, and 8251027501000010). Part of the synthesis was conducted at SUNY Binghamton and supported by NSF DMR-0731382.

Notes and references

1 A. R. West, *Solid State Chemistry and its Application*, John Willey & Sons Ltd, New York, 1994.
2 Y. W. Jun, J. S. Choi and J. Cheon, *Angew. Chem., Int. Ed.*, 2006, **45**, 3414; C. Burda, X. B. Chen, R. Narayanan and M. A. El-Sayed, *Chem. Rev.*, 2005, **105**, 1025; G. Ozin and A. Arsenault, *Nanochemistry: A Chemical Approach to Nanomaterials*, RSC Publishing, Cambridge, 2005.
3 X. G. Zhang, X. Ge and C. Wang, *Cryst. Growth Des.*, 2009, **9**, 4301; L. M. Shen, N. Z. Bao, Y. Q. Zheng, A. Gupta, T. C. An and K. Yanagisawa, *J. Phys. Chem. C*, 2008, **112**, 8809; P. Ptacek, H. Schafer, K. Kompe and M. Haase, *Adv. Funct. Mater.*, 2007, **17**, 3843.
4 Q. J. Feng, D. Z. Shen, J. Y. Zhang, B. S. Li, B. H. Li, Y. M. Lu, X. W. Fan and H. W. Liang, *Appl. Phys. Lett.*, 2006, **88**, 012505.
5 K. W. Liu, J. Y. Zhang, D. Z. Shen, C. X. Shan, B. H. Li, Y. M. Lu and X. W. Fan, *Appl. Phys. Lett.*, 2007, **90**, 262503; X. J. Wu, Z. Z. Zhang, J. Y. Zhang, Z. G. Ju, B. H. Li, B. S. Li, C. X. Shan, D. X. Zhao, B. Yao and D. Z. Shen, *Thin Solid Films*, 2008, **516**, 6116.
6 M. Z. Xue and Z. W. Fu, *Acta Chim. Sinica*, 2007, **65**, 2715.
7 Y. Takemura, H. Suto, N. Honda and K. Kakuno, *J. Appl. Phys.*, 1997, **81**, 5177.
8 X. J. Wu, D. Z. Shen, Z. Z. Zhang, J. Y. Zhang, K. W. Liu, B. H. Li, Y. M. Lu, B. Yao, D. X. Zhao, B. S. Li, C. X. Shan, X. W. Fan, H. J. Liu and C. L. Yang, *Appl. Phys. Lett.*, 2007, **90**, 112105.
9 X. J. Wu, Z. Z. Zhang, J. Y. Zhang, Z. G. Ju, D. Z. Shen, B. H. Li, C. X. Shan and Y. M. Lu, *J. Cryst. Growth*, 2007, **300**, 483.
10 F. C. Hsu, J. Y. Luo, K. W. Yeh, T. K. Chen, T. W. Huang, P. M. Wu, Y. C. Lee, Y. L. Huang, Y. Y. Chu, D. C. Yan and M. K. Wu, *Proc. Natl. Acad. Sci. U. S. A.*, 2008, **105**, 14262–14264.
11 H. Kotegawa, S. Masaki, Y. Awai, H. Tou, Y. Mizuguchi and Y. Takano, *J. Phys. Soc. Jpn.*, 2008, **77**, 113703; Y. Mizuguchi, F. Tomioka, S. Tsuda, T. Yamaguchi and Y. Takano, *Appl. Phys. Lett.*, 2008, **93**, 152505; D. Braithwaite, B. Salce, G. Lapertot, F. Bourdarot, C. Marin, D. Aoki and M. Hanfland, *J. Phys.: Condens. Matter*, 2009, **21**, 232202; L. Li, Z. R. Yang, M. Ge, L. Pi, J. T. Xu, B. S. Wang, Y. P. Sun and Y. H. Zhang, *J. Supercond. Novel Magn.*, 2009, **22**, 667; S. Margadonna, Y. Takabayashi, Y. Ohishi, Y. Mizuguchi, Y. Takano, T. Kagayama, T. Nakagawa, M. Takata and K. Prassides, *Phys. Rev. B: Condens. Matter Mater. Phys.*, 2009, **80**, 064506; J. N. Millican, D. Phelan, E. L. Thomas, J. B. Leao and E. Carpenter, *Solid State Commun.*, 2009, **149**, 707; V. A. Sidorov, A. V. Tsvyashchenko and R. A. Sadykov, *J. Phys.: Condens. Matter*, 2009, **21**, 415701.
12 T. M. McQueen, Q. Huang, V. Ksenofontov, C. Felser, Q. Xu, H. Zandbergen, Y. S. Hor, J. Allred, A. J. Williams, D. Qu, J. Checkelsky, N. P. Ong and R. J. Cava, *Phys. Rev. B: Condens. Matter Mater. Phys.*, 2009, **79**, 014522.

13 S. Medvedev, T. M. McQueen, I. A. Troyan, T. Palasyuk, M. I. Eremets, R. J. Cava, S. Naghavi, F. Casper, V. Ksenofontov, G. Wortmann and C. Felser, *Nat. Mater.*, 2009, **8**, 630–633.
14 M. J. Wang, J. Y. Luo, T. W. Huang, H. H. Chang, T. K. Chen, F. C. Hsu, C. T. Wu, P. M. Wu, A. M. Chang and M. K. Wu, *Phys. Rev. Lett.*, 2009, **103**, 117002; Y. F. Nie, E. Brahimi, J. I. Budnick, W. A. Hines, M. Jain and B. O. Wells, *Appl. Phys. Lett.*, 2009, **94**, 242505.
15 K. D. Oyler, X. L. Ke, I. T. Sines, P. Schiffer and R. E. Schaak, *Chem. Mater.*, 2009, **21**, 3655.
16 J. Yang, G. H. Cheng, J. H. Zeng, S. H. Yu, X. M. Liu and Y. T. Qian, *Chem. Mater.*, 2001, **13**, 848; A. P. Liu, X. Y. Chen, Z. J. Zhang, Y. Jiang and C. W. Shi, *Solid State Commun.*, 2006, **138**, 538; Y. Xie, L. Y. Zhu, X. C. Jiang, J. Lu, X. W. Zheng, W. He and Y. Z. Li, *Chem. Mater.*, 2001, **13**, 3927.
17 A. J. Williams, T. M. McQueen and R. J. Cava, *Solid State Commun.*, 2009, **149**, 1507–1509; B. C. Sales, A. S. Sefat, M. A. McGuire, R. Y. Jin, D. Mandrus and Y. Mozharivskyj, *Phys. Rev. B: Condens. Matter Mater. Phys.*, 2009, **79**, 094521.
18 B. H. Mok, S. M. Rao, M. C. Ling, K. J. Wang, C. T. Ke, P. M. Wu, C. L. Chen, F. C. Hsu, T. W. Huang, J. Y. Luo, D. C. Yan, K. W. Ye, T. B. Wu, A. M. Chang and M. K. Wu, *Cryst. Growth Des.*, 2009, **9**, 3260; S. B. Zhang, X. D. Zhu, H. C. Lei, G. Li, B. S. Wang, L. J. Li, X. B. Zhu, Z. R. Yang, W. H. Song, J. M. Dai and Y. P. Sun, *Supercond. Sci. Technol.*, 2009, **22**, 075016.
19 U. Patel, J. Hua, S. H. Yu, S. Avci, Z. L. Xiao, H. Claus, J. Schlueter, V. V. Vlasko-Vlasov, U. Welp and W. K. Kwok, *Appl. Phys. Lett.*, 2009, **94**, 082508.
20 Y. J. Xia, F. Q. Huang, X. M. Xie and M. H. Jiang, *Europhys. Lett.*, 2009, **86**, 37008.
21 P. Curie, *Bull. Soc. Fr. Mineral. Cristallogr.*, 1885, **8**, 145; G. Z. Wulff, *Kristallogr.*, 1901, **34**, 449.
22 J. Zhang and J. Y. Fang, *J. Am. Chem. Soc.*, 2009, **131**, 18543; M. Chen, J. Kim, J. P. Liu, H. Y. Fan and S. H. Sun, *J. Am. Chem. Soc.*, 2006, **128**, 7132.
23 D. Xu, Z. P. Liu, H. Z. Yang, Q. S. Liu, J. Zhang, J. Y. Fang, S. Z. Zou and K. Sun, *Angew. Chem., Int. Ed.*, 2009, **48**, 4217.